CHEMISTRY
A European Journal

Supporting Information

Enhancing Metal Separations by Liquid–Liquid Extraction Using Polar Solvents

Zheng Li,[a] Zidan Zhang,[a] Simon Smolders,[b] Xiaohua Li,[a] Stijn Raiguel,[a] Erik Nies,[a] Dirk E. De Vos,[b] and Koen Binnemans*[a]

chem_201901800_sm_miscellaneous_information.pdf

1. EXPERIMENTAL MATERIALS AND METHODS

1.1 Chemicals

$CoCl_2 \cdot 6H_2O$ (analytical grade), $EuCl_3 \cdot 6H_2O$ (99.99%), $YCl_3 \cdot 6H_2O$ (99.9%), $MnCl_2$ (97%), ethylene glycol (99.9%) and formic acid (>99%) were purchased from Acros Organics (Geel, Belgium); $NiCl_2 \cdot 6H_2O$ (97%), formamide (99%) and Ga standard solution (1000 ± 10 mg/L) were purchased from Chem-Lab (Zedelgem, Belgium); Aliquat® 336 (~90%), acetonitrile-d_3 (99.9%), methanol-d_4 and Triton™ X-100 (for molecular biology) were obtained from Sigma–Aldrich (Diegem, Belgium); Cyphos® IL 101 (>97%) was purchased from Cytec Industries Inc. (Niagara Falls, Ontario, Canada); $LaCl_3 \cdot 7H_2O$ (99.99%), $GdCl_3 \cdot 6H_2O$ (99.9%), *N*-methylformamide (99%) were obtained from Alfa Aesar (Karlsruhe, Germany); methanol (analytical reagent), ethanol (analytical reagent), isopropanol (analytical reagent), dimethyl sulfoxide (analytical reagent) and LiCl (analytical reagent grade) were supplied by Fisher Scientific (Merelbeke, Belgium); $SmCl_3 \cdot 6H_2O$ (99.9%), $PrCl_3 \cdot 7H_2O$ (99.9%), $NdCl_3 \cdot 6H_2O$ (99.9%) and $YbCl_3 \cdot 6H_2O$ (99.9%) were obtained from Strem Chemicals (Newburyport, USA); toluene (99.5%) and acetic acid (100%) were purchased from VWR Chemicals (Leuven, Belgium); $DyCl_3 \cdot 6H_2O$ (99.9%) was purchased from abcr GmbH (Karlsruhe, Germany); a silicone solution in isopropanol for the treatment of the TXRF quartz glass carriers was obtained from SERVA Electrophoresis GmbH (Heidelberg, Germany). Milli-Q water (18.2 MΩ·cm at 298.2 K) was used to prepare the aqueous solutions. All chemicals were used as received, without any further purification.

1.2 Experimental procedures

Solvent extraction. 10 vol% A336 (~0.2 M) dissolved in toluene was used as the less polar (LP) phase. The concentration of each transition metal salt ($MnCl_2$, $CoCl_2$ and $NiCl_2$) was 0.01 M and the $LaCl_3$ concentration was 8.3×10^{-4} M in the initial more polar (MP) phases. The ratio of Ni/La was based on the ratio in the nickel-metal hydride batteries.[1,2] The concentration of LiCl in the MP phase varied from 0.0 M up to saturation in each polar solvent. For each extraction experiment, 5.0 mL of MP phase and 5.0 mL of LP phase were contacted with each other in a 15 mL centrifuge tube and shaken on a table shaker (Thermo Scientific MaxQ 2000) at 260 rpm for 30 min at room temperature. In spite of easy phase disengagement for most samples, all the samples were centrifuged at 4000 rpm for 5 min (Eppendorf Centrifuge 5804) after shaking.

The percentage extraction *%E*, distribution ratio *D* and separation factor α are defined below:

$$\%E = \frac{c_{lp} \cdot V_{lp}}{c_{lp} \cdot V_{lp} + c_{mp} \cdot V_{mp}} \times 100\% \quad \text{(S1)}$$

$$D = \frac{c_{lp}}{c_{mp}} \quad \text{(S2)}$$

$$\alpha = \frac{D_A}{D_B} \quad \text{(S3)}$$

where c_{lp} and c_{mp}, V_{lp} and V_{mp} are concentrations and volumes in the LP phase and the MP phase, respectively; D_A and D_B are the distribution ratios of metals A and B respectively. The volume change after equilibrium due to mutual solubility of the two phases was taken into consideration in Eq. (S1).

Mutual solubility. The polar solvents with varying LiCl concentrations were contacted with 10 vol % A336 diluted in toluene with a phase ratio of 2.0 mL: 2.0 mL and shaken on a table shaker at 260 rpm for 30 min at room temperature, followed by centrifugation at 4000 rpm for 5 min. The ^{1}H NMR spectra of the LP phases were recorded directly with acetonitrile-d_3 or methanol-d_4 as solvent when appropriate for avoidance of signal overlapping. The MP phases were diluted by dimethylformamide or methanol (as reference) before recording their ^{1}H NMR spectra. The solubilities were calculated based on the compositions in each phase.

5.0 mL of each polar solvent with saturated LiCl (13.0 M LiCl in water, 4.0 M LiCl in EG, 6.0 M LiCl in formamide, 5.4 M LiCl in NMF and 7.0 M LiCl in methanol) and 5.0 mL of LP phase (10 vol% A336 in toluene) was contacted and shaken on a table shaker at 260 rpm for 30 min at room temperature, followed by centrifugation at 4000 rpm for 5 min. Subsequently, 3.0 mL of the clear LP phase was taken out and contacted with 3.0 mL of 1.0 M HCl aqueous solution and shaken for 30 min, followed by centrifugation. The resultant aqueous solutions were then diluted and measured by ICP-OES for Li^I concentration. The tests were carried out in duplicates.

1.3 Analytical instruments

The metal concentrations in both phases were measured by a TXRF spectrometer (Bruker S2 Picofox). Samples from both the LP phase and the MP phase were diluted with a mixture of aqueous Triton^{TM} X-100 solution and ethanol with Ga standard solution as reference to an appropriate concentration. The quartz glass sample carriers for TXRF measurements were pretreated with 30 µL of a silicone solution in isopropanol and dried in oven for 5 min at 333 K. Then, a diluted sample of 5 µL was added to a carrier and dried at 333 K for 30 min. Each sample was measured for 500 s in the TXRF spectrometer. The water content in the LP phase after equilibrium with aqueous solutions containing various LiCl concentration was determined by a Karl Fischer Coulometer (Mettler-Toledo C30S). Electron paramagnetic resonance (EPR) spectra were recorded at 140 K on a Bruker 300E continuous wave spectrometer with a rectangular cavity. The samples were irradiated with a microwave frequency of 9.739 MHz. UV-VIS absorption spectra were measured by a Varian Cary 5000 spectrophotometer using a pair of quartz cuvettes (10.0 mm path length). The steady-state photoluminescence measurements were performed on an Edinburgh Instruments FLS980, with a 450 W xenon lamp as light source and a red-sensitive photomultiplier tube (Hamamatsu 928P). The emission spectra were measured between 500 and 750 nm, the excitation wavelength was λ=394 nm. The ^{1}H NMR spectra were recorded by a Bruker Avance 400 spectrometer operating at 400 MHz, the ^{139}La and ^{35}Cl NMR spectra were recorded by a Bruker Avance 600 spectrometer operating at 85 MHz and 59 MHz, respectively. D_2O was used as an external reference in a coaxial insert within the NMR tube for locking the frequency

when recording the ^{35}Cl and ^{139}La NMR spectra. The parameters for ^{35}Cl spectrum recording were: 500 ppm sweep width with middle of spectrum at O1P 50 ppm; D1 delay between scans was 0.5 sec; 16 scans; pulse program was zg. The parameters for ^{139}La spectrum recording were: 1000 ppm sweep width with middle of spectrum at O1P 140 ppm; D1 delay between scans was 0.5 sec; 32 scans; pulse program was zg.

1.4 DFT calculations

The Density Functional Theory (DFT) calculations were performed using the Gaussian ver. 09 program.[3] The ground-state geometrical optimizations and analyses were calculated under BHandHLYP level of theory in conjunction with the DEF2SVP basis set,[4,5] which had been proven to give reliable results in similar systems with the consideration of accuracy and efficiency.[6] In order to validate the optimized structures and obtain the Gibbs free energy values, the vibrational frequency calculations were further executed.

2. RESULTS AND DISCUSSIONS

2.1. DFT calculations

Ten different polar solvents (acetic acid, isopropanol, ethanol, methanol, ethylene glycol (EG), dimethyl sulfoxide (DMSO), formic acid, water, formamide and *N*-methylformamide (NMF)) with their dielectric constants ranging from 6.25 to 181.56 were selected to investigate the influence of solvent effects on the binding energy (E_{binding}) of anionic chlorometallate complex.

$$E_{binding} = E_{[MCl_4]^{n-4}} - E_{M^{n+}} - 4E_{Cl^-} \quad \text{(S4)}$$

where M^{n+} is a cation with valence of *n*. The polarizable continuum model was used for the solvent effect calculations. As shown in Fig. S2, the binding energy of these metals becomes less negative with increasing dielectric constant of solvents and varies by more than 300 kJ·mol^{-1} for each metal.

Five solvents (methanol, EG, water, formamide and NMF) were selected as suitable candidates for solvent extraction applications. The solvation energy ($E_{\text{solvation}}$) of Co^{II} in these solvents considering the first coordination sphere was further computed with solvent effects taken into account using the polarizable continuum model.

$$E_{solvation} = E_{[Co(S)_x]^{2+}} - xE_S - E_{Co^{2+}} \quad \text{(S5)}$$

where *x* is the number of ligands, *x* = 3 for EG and *x* = 6 for all other solvents. All the coordination structures are based on reported experimental studies.[7–17] The solvation energy of Co^{II} in these solvents varies by about 180 kJ·mol^{-1} (Fig. S3). The solvation with EG is the weakest, because only three molecules are involved in the solvation since it is bidentate, whereas six molecules are required in the solvation for monodentate solvents. Among all the monodentate solvents, interestingly, the larger the molecule, the stronger the solvation energy.

2.2 Molarity concentrations of polar solvents

Since the extraction reaction involves the solvation of metals, the molarity concentration of polar solvents plays a role in the reaction equilibrium. On the basis of physicochemical properties of these polar solvents, the molarity concentrations were calculated (Table. S1). The concentration range is sufficient to affect extraction equilibrium.

2.3 Solvent sequence for $[CoCl_4]^{2-}$ formation

The efficiency for $[CoCl_4]^{2-}$ formation in ten different polar solvents were determined and compared according to the concentrations of $CoCl_2$ and LiCl required to reach the same absorbance (*e.g.* ~1.5 at 691 nm, Fig. S4). The more $CoCl_2$ and LiCl required to reach a certain absorbance, the less efficient the $[CoCl_4]^{2-}$ formation in the solvent. Interestingly, water is the least efficient solvent since it requires the highest $CoCl_2$ and LiCl, although it is the most commonly used solvent. Formamide is slightly more efficient than EG; both formamide and EG are more efficient than water and less efficient than the other seven solvents in Fig. S4-c, which follow the sequence of dimethyl sulfoxide (DMSO) > *N*-methylformamide (NMF) ≈ formic acid ≈ acetic acid ≈ isopropanol > ethanol > methanol. Five polar solvents have been identified as suitable candidates for liquid-liquid extraction because they can form two immiscible phases with the LP phase. The sequence of their efficiency for $[CoCl_4]^{2-}$ formation is: *N*-methylformamide (NMF) > methanol > formamide > EG > water.

To compare the formation efficiency of $[CoCl_4]^{2-}$ in different solvents, we can either keep the concentration of metals and salts the same in all polar solvents and compare the intensity of absorption, or we can keep the intensity of absorption the same and compare the concentration of metal (or salts) required. The first method seems more straightforward, however, it is not convenient in this study because the efficiency for $[CoCl_4]^{2-}$ formation in different polar solvent varies so much that the intensity of the absorption spectra spans over two orders of magnitudes, consequently the spectra cannot be nicely presented together in one figure. Therefore, we chose the second method for presentation of results.

2.4 Water content

Water content in the LP phase decreases with the increasing LiCl concentration in the aqueous solution due to the decreasing water activity (Fig. S5). However, the extraction of Ni^{II} by A336 increases with increasing LiCl concentration. This is due to the fact that with increasing LiCl concentration, (1) the formation of $[NiCl_4]^{2-}$ is stronger due to more available chloride ions; (2) the salting-out effect is stronger for $[NiCl_x(H_2O)_{6-x}]^{2-x}$ due to higher ionic strength (more discussions in section 2.6 on "Ni^{II} extraction mechanism").

The solubility of A336 in water at 30 °C is only 1.2 $g \cdot L^{-1}$.[18] The solubility of A336 in the aqueous LiCl solutions after equilibrating with 10 vol% A336 is negligible.

2.5 Mutual solubility of the two phases

The solubility of A336 in polar solvents and the solubilities of polar solvents in the LP phase are shown in Fig. S6. The sequence of polar solvents in terms of the solubility of A336 is the same as the sequence based on $[CoCl_4]^{2-}$ formation: NMF > methanol > formamide > EG > water. Higher A336 solubility in a polar solvent makes the LP phase lose extractant, and consequently makes the extraction of metals to the LP phase less efficient. The polar solvents are quite soluble in the LP phase, however, the dissolved polar solvents do not necessarily enhance the extraction of the solvated metals. For example, up to 50 $g \cdot L^{-1}$ EG is soluble in the LP phase, but Ni^{II} is not extracted at all from the EG solution.

Compared with solvent extraction systems with an aqueous phase, non-aqueous solvent extraction systems have larger mutual solubility of the two phases. The mutual solubility can be decreased by multiple measures, such as selecting suitable diluent and solvent pairs and addition of salts (*e.g.* LiCl) in the polar solvents. Despite of the relatively large uptake of polar solvents into the less polar phase in some cases, once the mutual solubility equilibrium is reached, in the following operations (*e.g.* extraction and stripping), the mutual solubility remains largely unchanged. According to our observations so far, the dissolved polar solvents in the less polar phase behave similarly as a diluent, *i.e.* they are not involved in the coordination, hence not posing significant issues in metal separations.

Extraction of Li^{I} into the LP phase from polar solvents with saturated LiCl (13.0 M LiCl in water, 4.0 M LiCl in EG, 6.0 M LiCl in formamide, 5.4 M LiCl in NMF and 7.0 M LiCl in methanol) was determined to be 0.89, 0.10, 0.13, 0.23 and 1.91 $g \cdot L^{-1}$ Li^{I} (not LiCl), respectively. Extraction of Li^{I} is relatively high when methanol and water was used as polar solvents. This observation is the same as the extraction of La^{III} from these solvents (Fig. 3). Extraction of Li^{I} from all solvents was smaller than 1% of the initial amount except for when methanol was the solvent, in which case the extraction of Li^{I} was about 3.9%.

2.6 Ni^{II} extraction mechanism

The extraction of $CoCl_2$ and $MnCl_2$ by A336 are known to proceed by forming the anionic chlorometallate complexes that bind to the alkyl ammonium cations, but the extraction of $NiCl_2$ warrants further investigation. We first extracted $NiCl_2$ from the aqueous solutions with 0.01 M $NiCl_2$ and 9.0 M and 12.0 M LiCl, respectively, and from the methanolic solution with 0.01 M $NiCl_2$ and 6.0 M LiCl, using 10 vol% A336 dissolved in toluene. The loaded LP phases were diluted to have the same Ni^{II} concentration (after measuring by TXRF) and then the UV-VIS absorption spectra were measured by a Varian Cary 5000 spectrophotometer using a pair of quartz cuvettes (10.0 mm path length). (Fig. S7). We can see that the concentration of $[NiCl_4]^{2-}$ in the LP phases loaded from the aqueous solution with 12.0 M LiCl and that loaded from the methanolic solution with 6.0 M LiCl are the same, whereas, the concentration of $[NiCl_4]^{2-}$ in the LP phase loaded from the aqueous solution with 9.0 M LiCl is much lower. This difference in $[NiCl_4]^{2-}$

concentration indicates that part of Ni^{II} is not extracted in the form of $[NiCl_4]^{2-}$ from the aqueous solution with 9.0 M LiCl. Then the initial $NiCl_2$ concentration in the three feed solutions was increased to 0.10 M and the A336 concentration was increased to 20 vol%. The UV-VIS spectra of the loaded phases were recorded again without dilution. Besides the absorption for $[NiCl_4]^{2-}$, the LP phase loaded from the aqueous solution with 9.0 M LiCl shows an absorption band at ~402 nm, which corresponds to the octahedral structure $[Ni(H_2O)_{6-x}Cl_x]^{2-x}$.[19] This octahedral species cannot be extracted by binding to alkyl ammonium cations since it is not anionic; it is most likely extracted by dissolving in the LP phase. The LP phase being able to accommodate the aquated Ni^{II} complex is because: (1) A336, as an ionic liquid, is polar, and toluene is also slightly polar; (2) A336 extracts water (Fig. S5), which facilitates the dissolution of the aquated complexes. This extraction mechanism is similar to the extraction of rare earths from chloride solutions by A336. Because rare earths have a low propensity to form chlorometallate complexes, they were extracted into the A336 phase in the form of aquated complexes.[20]

Therefore, Ni^{II} is extracted by A336 from the aqueous chloride solutions by two different mechanisms: (1) formation of $[NR_4]_2{\cdot}[NiCl_4]$ and (2) dissolving as solvation complexes. At low LiCl concentration, formation of $[NiCl_4]^{2-}$ is weak and dissolving as solvation complexes is the main extraction mechanism; at high LiCl concentration, formation of $[NR_4]_2{\cdot}[NiCl_4]$ dominates.

2.7 La^{III} extraction from aqueous solutions

$LaCl_3$ in the aqueous solution (without $NiCl_2$) was extracted by 10 vol% A336. The percentage extraction increases with the increasing LiCl concentration until 8.0 M LiCl and then decreases slightly (Fig. S8). This trend is the same as when $NiCl_2$ and $LaCl_3$ were extracted together (Fig. 3), thus the competition for extractant between $NiCl_2$ and $LaCl_3$ can be ruled out. The increase of $LaCl_3$ extraction is due to the increasing interactions with electrolytes (LiCl) in aqueous solution, the decrease might be attributed to the transition of $[La(H_2O)_9]^{3+}$ to $[La(H_2O)_8Cl]^{2+}$. In aqueous solution, the main species of $LaCl_3$ is $[La(H_2O)_9]^{3+}$,[21] however, $[La(H_2O)_8Cl]^{2+}$ may form at high Cl^- concentration.[22-24] ^{139}La NMR indicates the existence of chloro-bound La^{III} in the aqueous solution as discussed in the main text. Therefore, the existence of $[La(H_2O)_8Cl]^{2+}$ is supported.

The salting-out of cationic complexes might be described by thermodynamic models of electrolyte systems, such as the Pitzer model[25–27] and the electrolyte-NRTL model[28,29]. In these models, the interactions among ions are dependent on both ion concentration and charge of ions, the higher ion concentration and the higher charge, the stronger interaction. In the extraction of La^{III}, the lower charge of $[LaCl(H_2O)_9]^{2+}$ compared to that of $[La(H_2O)_9]^{3+}$ may lead to weakening of the interaction, resulting in lower extraction. On the other hand, water content in the less polar phase decreases as the LiCl concentration increases. The lower water content may also reduce the capability of the LP phase for dissolving the aquated La^{III} complex.

2.8 La^{III}/Ni^{II} extraction from water and methanol mixtures

The extraction of La^{III} and Ni^{II} from mixtures of water and methanol with 5.0 M LiCl is presented in Fig. S9. The extraction of La^{III} decreases first and then increases with increasing water percentages. This trend is the same as the extraction from water and methanol mixtures with 9.0 M LiCl, and reflects the gradual transition of species from the solvation with methanol to the solvation with water. Both of the two solvation complexes can be extracted to the LP phase and the extraction from methanol is more efficient than from water. The extraction of Ni^{II} decreases quickly with addition of water due to the decreasing efficiency for the formation of $[NiCl_4]^{2-}$. When the water percentage is higher than 70 vol%, extraction of Ni^{II} slightly rises, which can be attributed to the extraction as solvation complexes with water. Noticeably, both the extractions of La^{III} and Ni^{II} by the two different mechanisms are sensitive to water content. With only 5 vol% water content, extraction of both La^{III} and Ni^{II} evidently decreases.

2.9 Extraction of Ni^{II} and La^{III}

There are generally three types of commercial extractants: (1) acidic extractants, such as alkyl carboxylic acids (*e.g.* Versatic 10: a mixture of carboxylic acids with the common structural formula of $C_{10}H_{20}O_2$) and organophosphorus acids (*e.g.* D2EHPA: di-(2-ethylhexyl)phosphoric acid); (2) neutral extractants, such as TBP (tributyl phosphate) and Cyanex 923 (a mixture of alkyl phosphine oxides); (3) basic extractants or anion exchangers, such as trioctylamine and Aliquat 336 (A336).

Acidic extractants have much higher affinity for La^{III} than Ni^{II} because of the higher charge density of La^{III}, hence La^{III} is always preferentially extracted over Ni^{II}.[30,31] Neither La^{III} nor Ni^{II} can be extracted by neutral extractants from aqueous chloride solutions, because both metals coordinate weakly to the chloride anions.[32,33] From the aqueous nitrate media, La^{III} can be efficiently extracted by neutral extractants,[34] while the extraction of Ni^{II} is very weak. Basic extractants (anion exchangers) usually extract metals by formation of anionic chlorometallate complexes. Since both La^{III} and Ni^{II} show little propensity to form anionic complex with chloride ions, the extraction for both metals is very low when HCl is used as chloride source.[35] When chloride salts, such as LiCl, are used as chloride source, La^{III} can be extracted by A336 via salting-out effect (extraction as solvation complex) as discussed in this study. Consequently it is difficult to leave La^{III} in the solution while extracting Ni^{II}. In short, no matter what kind of commercial extractant is used, Ni^{II} could not be preferentially extracted from La^{III} in aqueous solutions.

In addition to commercial extractants, some less common extractants were also studied for the extraction of Ni^{II} and La^{III}. A recent study showed that thiocyanate ionic liquids display good selectivity for the first-row d-block metals over rare-earth elements. The separation factor of Ni^{II}/La^{III} can be up to ~100,[36] which means, for example, about 10% La^{III} is co-extracted when about 90% Ni^{II} is extracted. This separation is inferior to the extraction system developed in this study, which extracts negligible La^{III} when about 80% Ni^{II} is extracted with a separation factor being almost infinite. More importantly, complete stripping of Ni^{II} from the loaded A336 can be

achieved by simply contacting with water, whereas the stripping of metals from loaded thiocyanate ionic liquids is difficult.

2.10 ^{35}Cl NMR spectra

^{35}Cl NMR spectra of aqueous $LaCl_3$ solutions are presented in Fig. S10. The free chloride anions in the aqueous solution of 0.10 M $LaCl_3$ without LiCl give a sharp peak and the shift is set as a reference at 0 ppm for all the ^{35}Cl NMR spectra. With addition of 6.0 M LiCl, the signal is shifted downfield, indicating that chloride ions are partially bound to La^{III}, because the signal is an average of the free chloride anions and bound chloride ions. This is an evidence for the existence of $[LaCl]^{2+}$. With the addition of 10.0 M LiCl, the peak is broader but the signal shifts back upfield. The disappearance of the downfield shift might be due to the free chloride anions being dominant. The ^{35}Cl signal in the loaded A336 phase was too weak for practical analysis.

^{35}Cl NMR spectra of methanolic solutions with 0.10 M $LaCl_3$ and various LiCl are presented in Fig. S11. The solution without LiCl has a downfield shift of about 71 ppm with respect to the reference (free chloride ions in aqueous solution) and the peak is broad, indicating that chloride ions are partially bound to La^{III}. This observation is consistent with the reports that the species in the methanolic La^{III} chloride solution is mainly $[LnCl_2]^+$ (methanol molecules are omitted).[37–41] Upon addition of LiCl, the shift is close to that of free chloride ions because the free chloride ions are dominant. The ^{35}Cl signal of the loaded A336 phase was too weak to be identified because there are no free chloride anions in this phase.

2.11 ^{139}La NMR spectra

To study the extraction mechanism, ^{139}La NMR spectra were recorded for the LP phase solutions and the corresponding aqueous raffinate solutions after extraction equilibrium, with initially 0.10 M $LaCl_3$ and 6.0 M (Fig. 4-d) or 8.0 M LiCl (Fig. S12) in the aqueous solution, respectively. 20 vol% A336 dissolved in toluene was used as the LP phase and a MP:LP ratio of 10 mL:2 mL was used to increase the loading of La^{III} to the LP phase in order to have better NMR signal. The spectra of the LP phase has the same shift as that of the aqueous solution but the band is less intense and broader. These observations show that the species in the LP phase is coordinated to more chloride ions than that in the corresponding aqueous solution. Comparing the ^{139}La NMR spectra of the less polar phases loaded from aqueous solution with 6.0 M and 8.0 M LiCl respectively, the later has a larger down-field shift, meaning that more chloride ions tend to coordinate with the extracted La^{III} at higher aqueous LiCl concentration and that La^{III} is extracted as a mixture. This observation is consistent with the results of Sm^{III} UV-Vis absorption spectra (Fig. 4-b).

The ^{139}La spectra of the methanolic solutions (Fig. S13) are broader and more downfield shifted compared to those of the aqueous solutions. Chloride ions coordinate more readily to La^{III} in methanol than in water, because water is a better ligand towards La^{III}, while chloride and methanol are similar. With addition of only 3.0 M LiCl almost all the La^{III} is bound to chloride ions as indicated by the disappearance of the ^{139}La NMR spectrum. The signal of ^{139}La in the LP phase

loaded from the methanolic solutions is too weak and broad to be clearly detected, because the signal of (partially) coordinated La^{III} is weak. Consequently, we cannot directly compare ^{139}La NMR spectra of the loaded LP phases and the corresponding methanolic solutions.

^{139}La NMR spectra of $LaCl_3$ in NMF (Fig. S14) show similar trend as those of $LaCl_3$ in water and in methanol (Fig. 4-c, S13): with the increasing LiCl concentration, the spectra broaden, shift downfield and the intensity decreases. These spectra features are the evidence of La^{III} binding with chloride ions. With 3.0 M LiCl, the ^{139}La spectrum almost disappears, indicating that La^{III} is almost completely bound to chloride ions. Comparing ^{139}La spectra in different solutions (Fig. 4-c, d and Fig. S12-S14), the shifts are largely different due to the coordination with different ligands (water, methanol, NMF and chloride ions).

2.12 Sm^{III} UV-VIS absorption spectra

The absorption spectra of 0.20 M $SmCl_3$ with various LiCl concentrations in water and methanol and the loaded LP phases (20 vol% A336 in toluene) were recorded with results shown in Fig. 4-a, b and S15−S18. The spectra of all the solutions have the same characteristic peaks except for small shifts (Fig. S15), which is an indication that the species in these solutions have similar coordination structures. $[Sm(H_2O)_9]^{3+}$ is the main species in the aqueous chloride solution of Sm^{III}. In the presence of methanol and chloride ions, possible structures are that water molecules in $[Sm(H_2O)_9]^{3+}$ are (partially) replaced by methanol molecules or chloride ions, forming species similar to the coordination structure of $[Sm(H_2O)_9]^{3+}$ but with lower symmetry.

For the spectra of methanolic solutions, similar red-shifts to the aqueous solutions are observed with increasing LiCl concentration (Fig. S16). It is interesting to note that, the absorption increases first and then decreases. The red-shifts and the change in the absorption intensity indicates the formation of at least three different $[SmCl_x]^{3-x}$ complexes. The absorption spectra of the loaded LP phase also show red-shifts (Fig. S18). Moreover, the peak location of the loaded LP phase is always more red-shifted than the methanolic solution (Fig. 4-b). By analogy to the case of extraction from aqueous solutions, the species in the loaded LP phase is a mixture and they are coordinated to more chloride ions than the corresponding species in the methanolic solutions. $[SmCl]^{2+}$ and $[SmCl_2]^{+}$ have been reported in methanolic solutions containing 0.09 M Sm^{III} on the basis of 2 nm red-shift of absorption spectra when 4.0 M $LiClO_4$ in the solution was gradually replaced by 4.0 M LiCl.[42] In this study, a red-shift of >3 nm was observed due to the higher Sm^{III} (0.20 M) and higher LiCl concentration (up to 6.0 M), which indicates further formation of the neutral $[SmCl_3]$. Considering that the main species of La^{III} in the methanolic chloride solutions has been consistently reported to be $[LaCl_2]^{+}$,[37–41] the species in the methanolic solution and the corresponding LP phases are likely $[LaCl]^{2+}$, $[LaCl_2]^{+}$ and $[LaCl_3]$.

Fig. S19 shows the spectra of the methanolic solutions before and after extraction and the spectra of the corresponding LP phases. With 4.0 M, 5.0 M and 6.0 M LiCl in the methanolic solutions, the extraction of Sm^{III} to the LP phase was 37%, 56% and 72% respectively. The higher Sm^{III} extraction to the LP phase, the higher red-shift of the spectra of the LP phase, moving from 406.5

nm at 4.0 M LiCl, to 407.0 nm and 407.2 nm at 5.0 and 6.0 M LiCl respectively. The red-shift of the spectra is an indication that more chloride ions are coordinated to Sm^{III} as the Sm^{III} concentration increases in the LP phase. Comparing the spectra of methanolic solutions before and after extraction, there is a slight blue-shift (~ 0.1 nm) for the spectra after extraction due to the lowering of Sm^{III} concentration. Despite that the extraction of Sm^{III} is high, the spectra shift is very small, because the high LiCl concentration in the methanolic solution provides abundant chloride ions, which probably could largely maintain the equilibrium among $[SmCl]^{2+}$, $[SmCl_2]^{+}$ and $[SmCl_3]$.

2.13 Gd^{III} EPR spectra

The methanolic solutions for EPR study contained 0.05 M $GdCl_3$ with varying LiCl concentrations. The 10 vol% A336 phase was loaded from the methanolic solution with 6.0 M LiCl. The Gd^{III} concentration in the A336 phase was determined by TXRF to be 0.034 M. EPR measurements were performed with a sweep width of 8900 G centered at 4500 G. Data were analyzed using the EasySpin software package.[43]

The EPR spectra of Gd^{III} in the methanolic solutions and the loaded LP phases are shown in Fig. S20. There are three distinct peaks visible in the spectrum of the Gd^{III} complexes in the loaded LP phase. These peaks with *g*-values of ~6.0, 2.8 and 2.0 are characteristic for a U-spectrum of Gd^{III} complexes.[44] This type of spectrum occurs often in glassy, disordered polycrystalline materials and its origin has been thoroughly investigated by Brodbeck and Iton.[45] A U-spectrum can be modeled using broadly distributed D-values with a maximum between 0.051 and 0.056 cm^{-1} and a distribution of E/D-values over the whole range of (0 – 1/3). The D and E/D values determine the symmetry of the complex: $D = 0$ indicates cubic symmetry; $D \neq 0$ and $E/D = 0$ means axial symmetry and $D \neq 0$ and $0 \leq E/D \leq 1/3$ means no symmetry. The broad distribution of D and E/D values indicate that low-symmetry, disordered Gd^{III}-complexes are formed. The EPR spectra of Gd^{III} in methanolic solutions have the same *g*-values and the same range of D and E/D values as the LP phase. Therefore, there is no significant difference in the symmetry of the Gd^{III} species in these solutions.

The EPR spectra of the undiluted loaded LP phase and the diluted solution (1:20) are further compared. Although the two spectra have the same peaks (Fig. S21), it is interesting to notice that the peak at $g = 2$ is much more intense in the undiluted sample and after subtraction, only that peak remains (the remaining peak at $g = 2.8$ might originate from a slight shift between the two spectra). This peak is often associated with a too high concentration of Gd^{III} or the presence of Gd^{III} clusters.[46]

2.14 Eu^{III} luminescence emission spectra

The emission spectra of $EuCl_3$ in methanol and in the loaded LP phases are presented in Fig. S22. Assignments of transitions with respect to wavelength have been given by Binnemans.[47] The spectra of methanolic solutions with 0.0, 2.0 and 6.0 M LiCl have shoulders for $^5D_0 \rightarrow {}^7F_2$

transitions (610−630 nm), which indicates the presence of two species in equilibrium. In fact, with the increase of LiCl concentration, more chloride ions would coordinate with Eu^{III} and multiple $[EuCl_x]^{3-x}$ species would be in equilibrium. Interestingly, with the increasing LiCl concentration, the intensity of $^5D_0 \rightarrow {}^7F_2$ transition increases, while the intensity of $^5D_0 \rightarrow {}^7F_4$ transition (680−710 nm) decreases. This change in intensity might be attributed to the increasing number of chloride ions coordinated to the Eu^{III} cation. Comparing the spectra of methanolic solutions with 4.0 M LiCl and 6.0 M LiCl with the corresponding loaded LP phases, the latter have higher intensity of $^5D_0 \rightarrow {}^7F_2$ transitions and lower intensity of $^5D_0 \rightarrow {}^7F_4$ transition. This difference in intensity is an indication that the species in the LP phases are coordinated to more chloride ions on average than that in the methanolic solutions. This inference is consistent with the UV-VIS spectra of Sm^{III} and ^{139}La NMR studies.

Görller-Walrand *et al*. studied the absorption spectra of $[EuCl_6]^{3-}$ in ethanol solutions using MCD (magnetic circular dichroism) and concluded that $[EuCl_6]^{3-}$ is a slightly distorted octahedral structure.[48] Eu^{III}-complexes having inversion centres would have a very low intensity for $^5D_0 \rightarrow {}^7F_2$ transition.[47] The high intensity of $^5D_0 \rightarrow {}^7F_2$ transition shown in the spectra proves that there is no $[EuCl_6]^{3-}$ present in either methanolic solutions or the loaded LP phases. This observation is consistent with results obtained from the UV-VIS spectra studies.

2.15 Extraction of rare-earth elements

Extraction curves of lanthanide chlorides from aqueous and methanolic solutions by A336 were established (Figs. S23 and S24). Comparing the two types of extraction isotherms, the extraction from aqueous solutions is suitable for the separation of heavy rare-earth elements from light rare-earths elements at high LiCl concentrations; the extraction from methanolic solutions is more suitable for the separation of neighboring elements at low LiCl concentration.

Table S1. Physicochemical properties of polar solvents

Solvents	Epsilon	MW ($g \cdot mol^{-1}$)	Density ($g \cdot mL^{-1}$) at 293.2 K	Concentration (M)
acetic acid	6.25	60.05	1.05	17.5
isopropanol	19.26	60.096	0.79	13.1
ethanol	24.85	46.069	0.79	17.1
methanol	32.61	32.042	0.79	24.7
ethylene glycol	40.25	62.068	1.11	17.9
dimethyl sulfoxide	46.83	78.129	1.10	14.1
formic acid	51.1	46.025	1.22	26.5
water	78.35	18.015	1.00	55.4
formamide	108.94	45.041	1.13	25.2
N-methylformamide	181.56	59.068	1.00	17.0

Note: Epsilon means dielectric constant and the data is from Gaussian.[49]

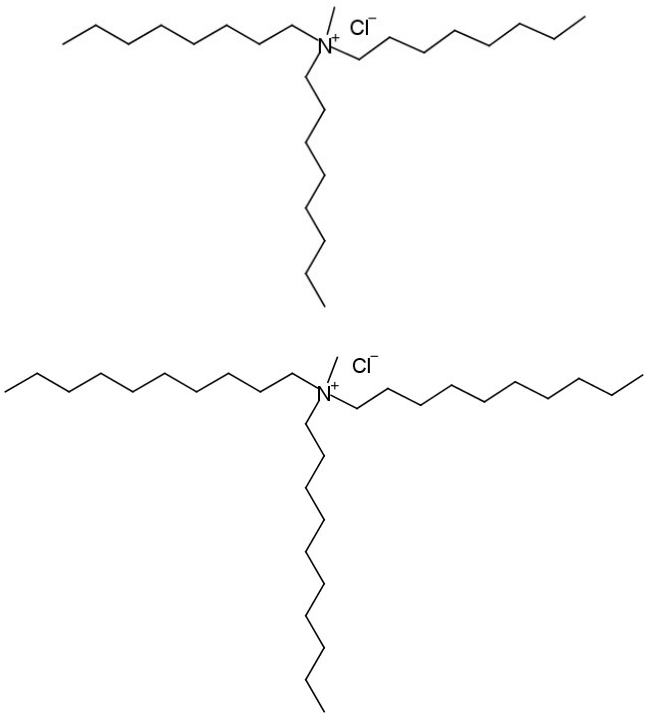

Figure S1. Structure of Aliquat 336 (A336): a mixture of methyltrioctylammonium chloride (predominating) and methyltridecylammonium chloride.

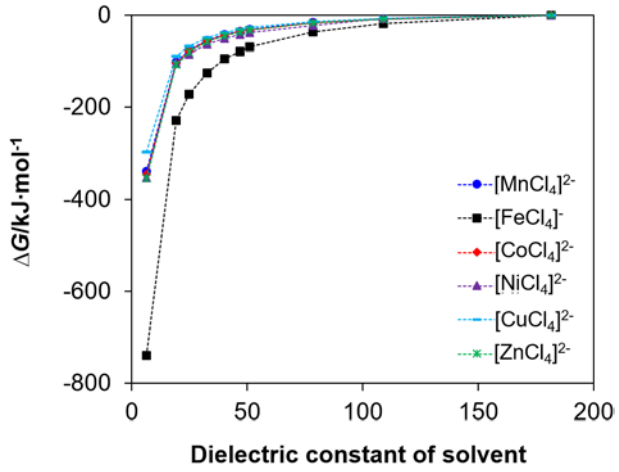

Figure S2. Dependence of binding energy on dielectric constant of polar solvents for six transition metal ions. *ΔG* presents the relative binding energy, which is obtained through Eq. S4 with the binding energy in NMF set as the benchmark (0 kJ·mol^{-1}) for each metal complex.

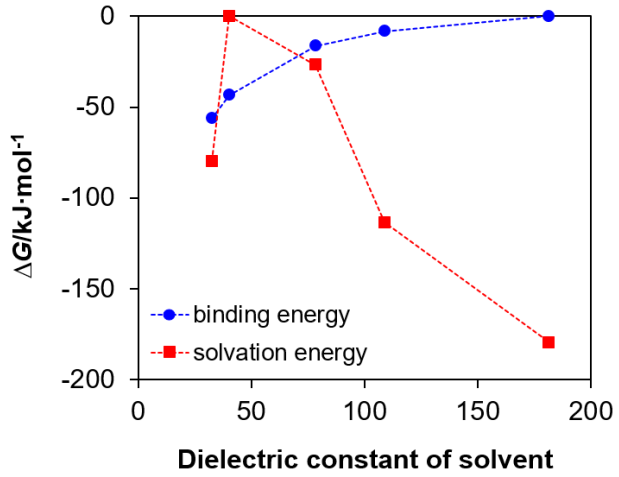

Figure S3. Binding energy of $[CoCl_4]^{2-}$ and solvation energy of Co^{II} in selected solvents with different dielectric constants (left to right: methanol, EG, water, formamide and NMF).

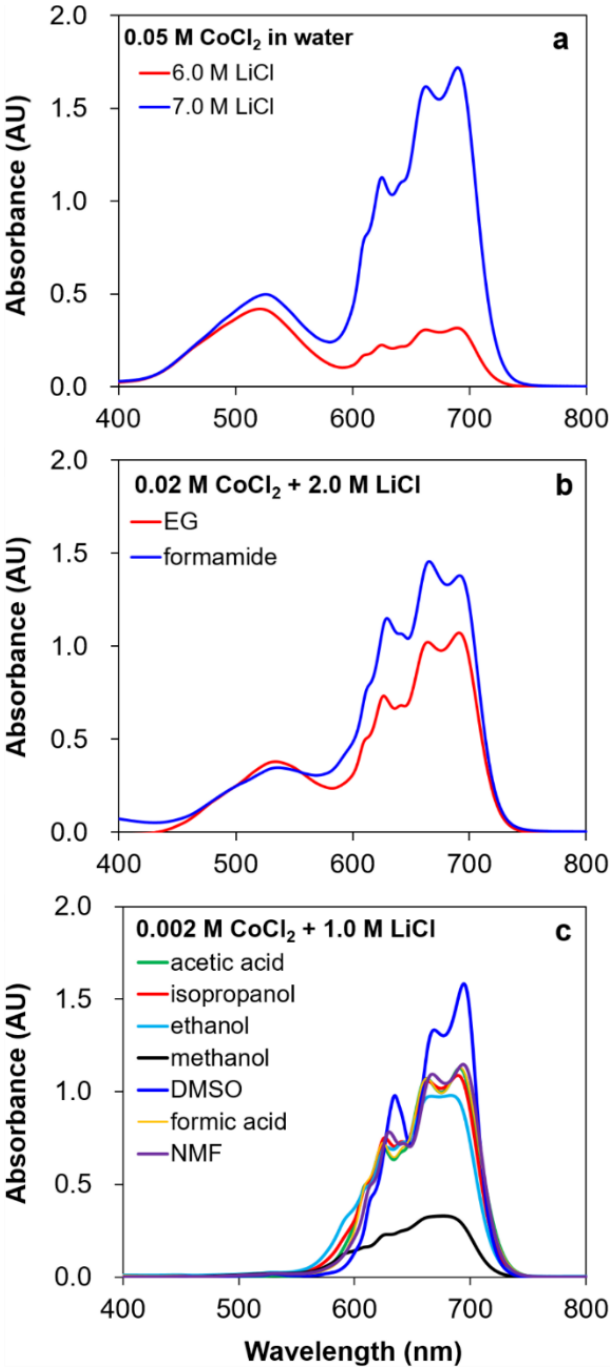

Figure S4. Formation of $[CoCl_4]^{2-}$ in ten polar solvents with various $CoCl_2$ and LiCl concentrations.

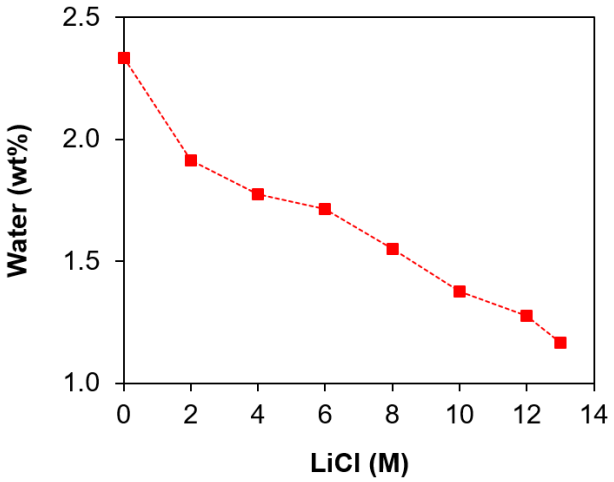

Figure S5. Water content in 10 vol% A336 after equilibrium with aqueous solutions containing various LiCl concentrations.

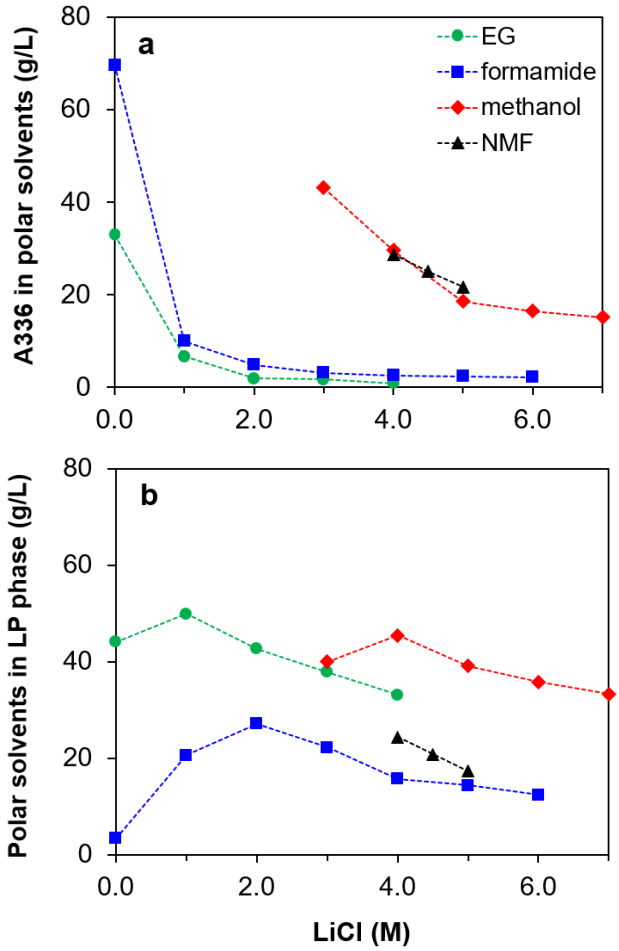

Figure S6. Mutual solubility of the LP phase (10 vol% A336 in toluene) and polar solvents (solubility of A336 in water is negligible).

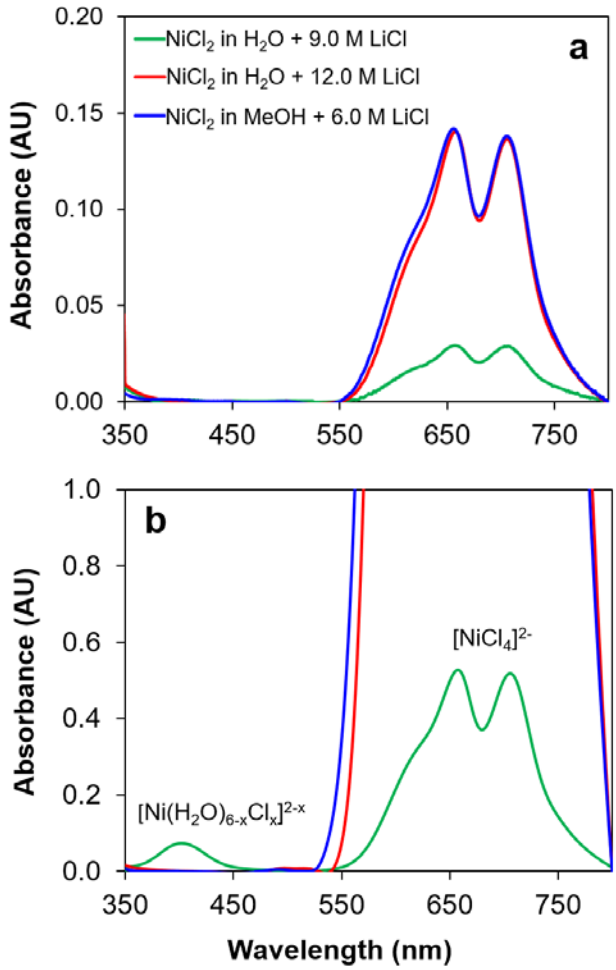

Figure S7. UV-VIS absorption spectra of Ni^{II} in the loaded LP phases: (a) 0.01 M $NiCl_2$ in MP phase, extracted by 10 vol% A336, the loaded LP phases were diluted to the same Ni^{II} concentration; (b) 0.10 M $NiCl_2$ in the MP phase, extracted by 20 vol% A336, the loaded LP phases were directly measured without dilution.

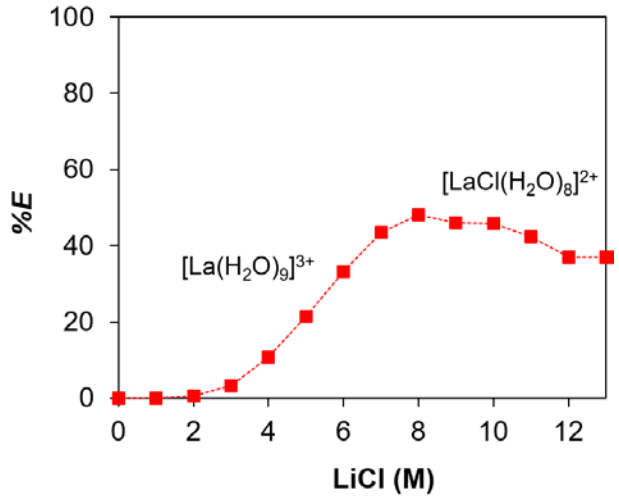

Figure S8. Extraction of La^{III} from aqueous solutions. MP phase: 8.3×10^{-4} M $LaCl_3$ in water with varying LiCl concentrations; LP phase: 10 vol% A336 in toluene.

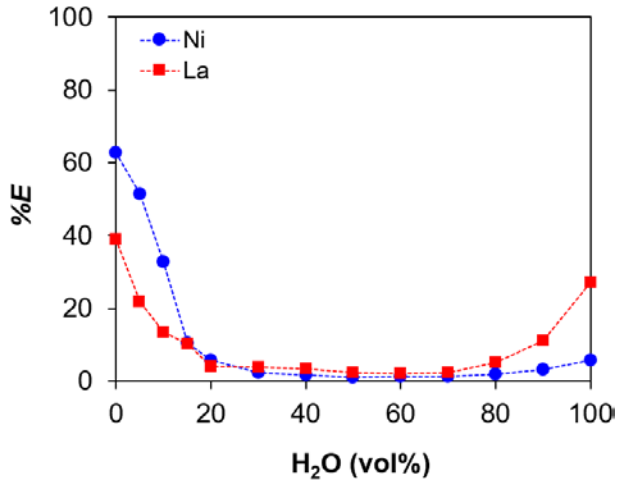

Figure S9. Extraction of La^{III}/Ni^{II} from mixtures of water and methanol. MP: 8.3×10^{-4} M $LaCl_3$ and 0.01 M $NiCl_2$ with 5.0 M LiCl in mixtures of water and methanol; LP phase: 10 vol% A336 in toluene.

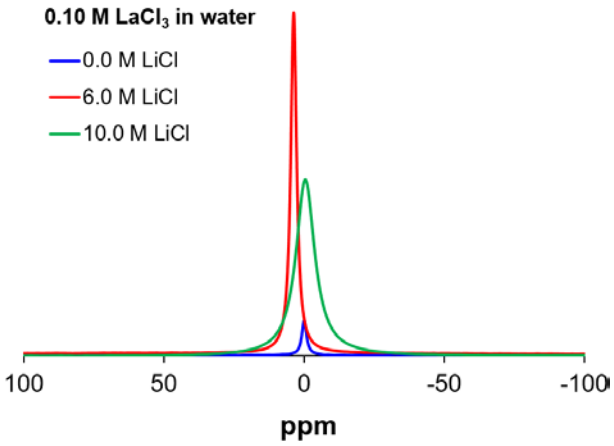

Figure S10. ^{35}Cl NMR spectra of 0.10 M La^{III} in aqueous solutions with various LiCl concentrations.

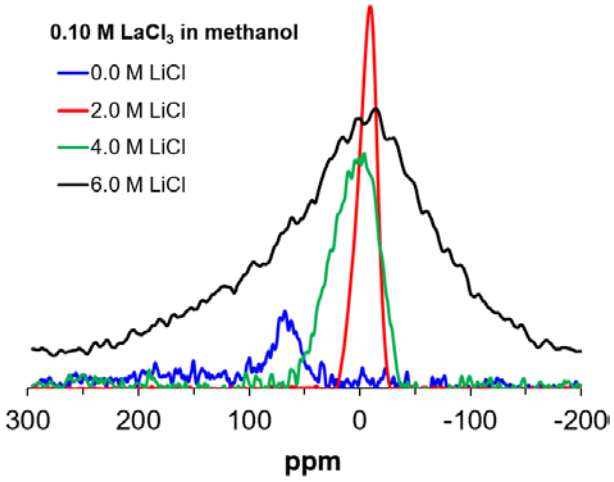

Figure S11. ^{35}Cl NMR spectra of 0.10 M La^{III} in methanolic solutions with various LiCl concentrations.

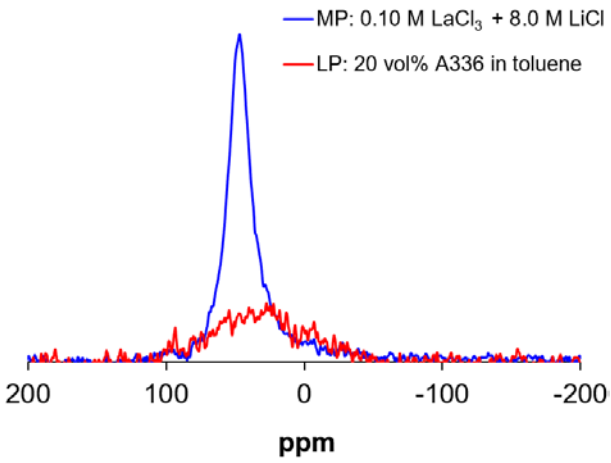

Figure S12. ^{139}La NMR spectra of an aqueous solution and the corresponding loaded LP phase.

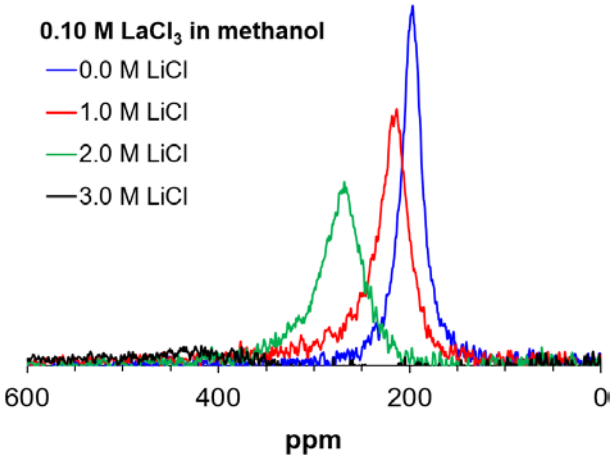

Figure S13. ^{139}La NMR spectra of La^{III} in methanolic solutions.

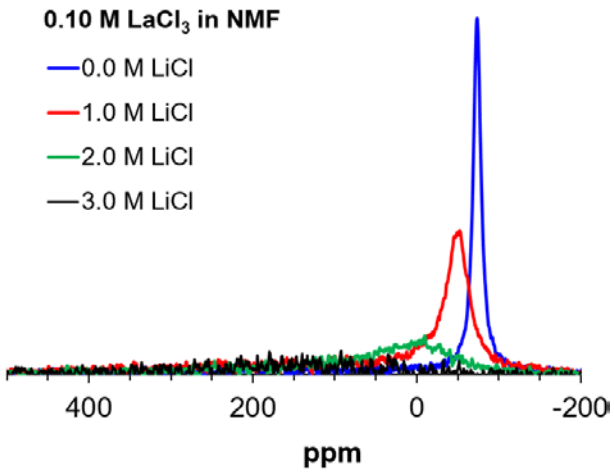

Figure S14. ^{139}La NMR spectra of La^{III} in NMF solutions.

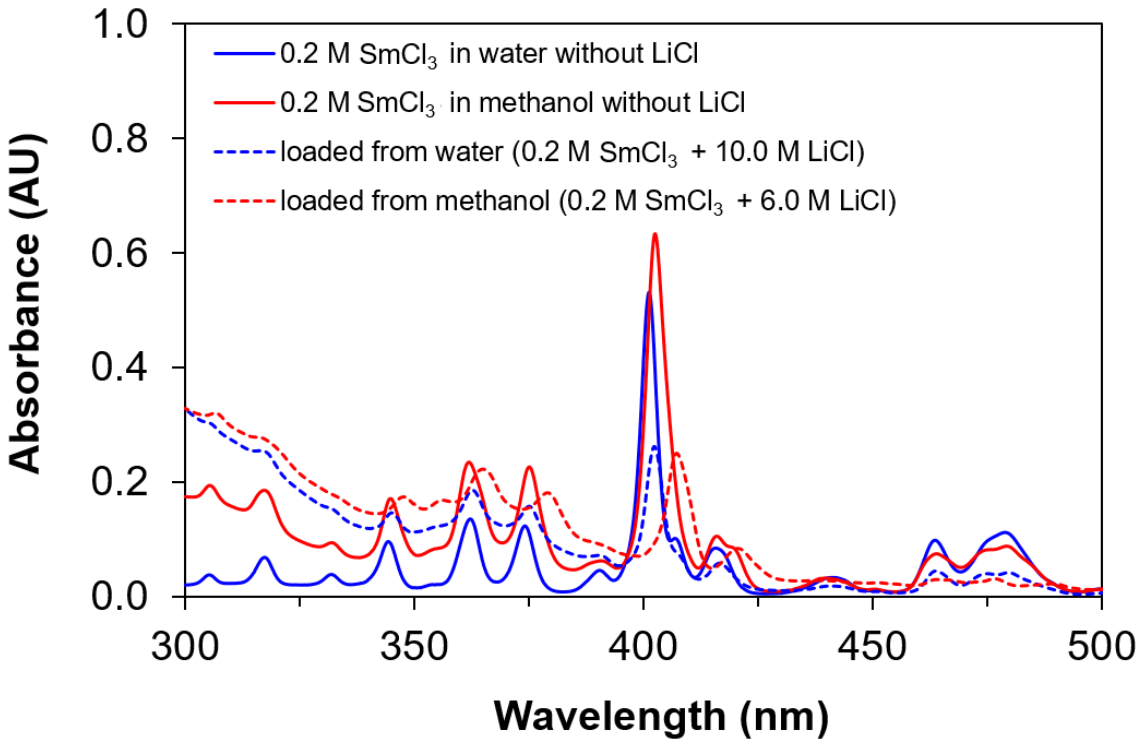

Figure. S15. UV-VIS absorption spectra of Sm^{III} in water, methanol and the loaded LP phases.

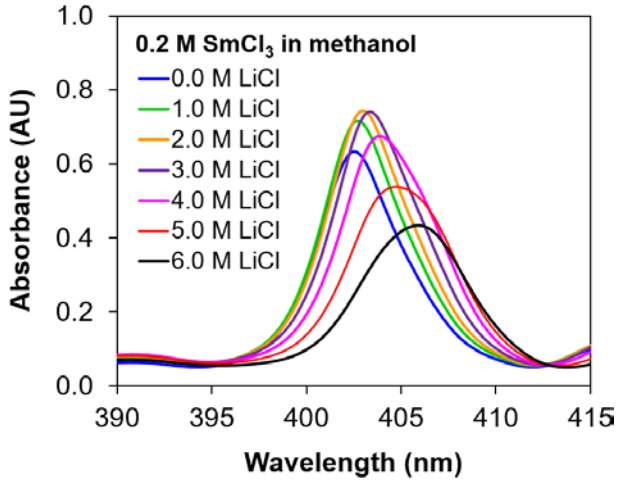

Figure S16. UV-VIS absorption spectra of Sm^{III} in methanolic solutions.

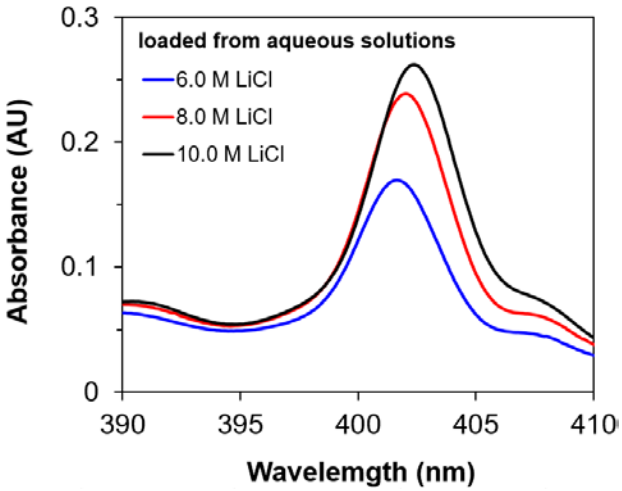

Figure S17. UV-VIS absorption spectra of Sm^{III} in LP phases loaded from aqueous solutions.

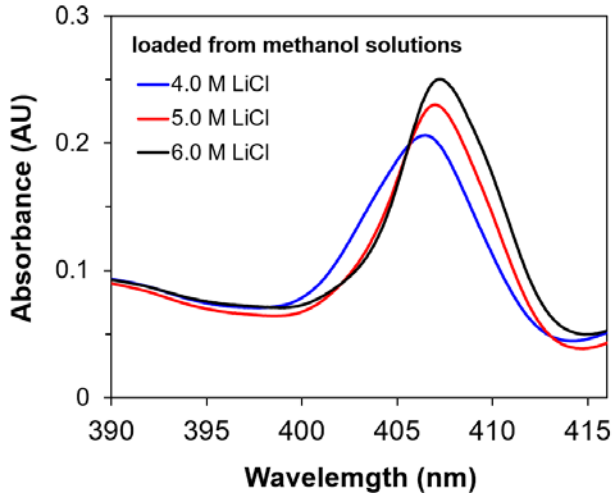

Figure S18. UV-VIS absorption spectra of Sm^{III} in LP phases loaded from methanolic solutions

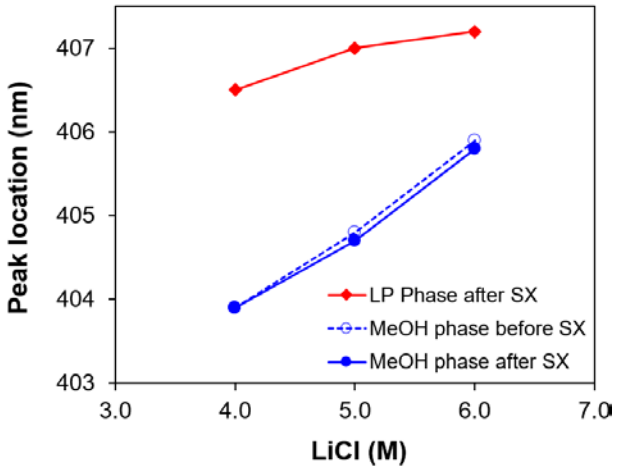

Figure S19. UV-VIS absorption spectra of Sm^{III} in LP phases and methanolic solutions before and after solvent extraction (SX).

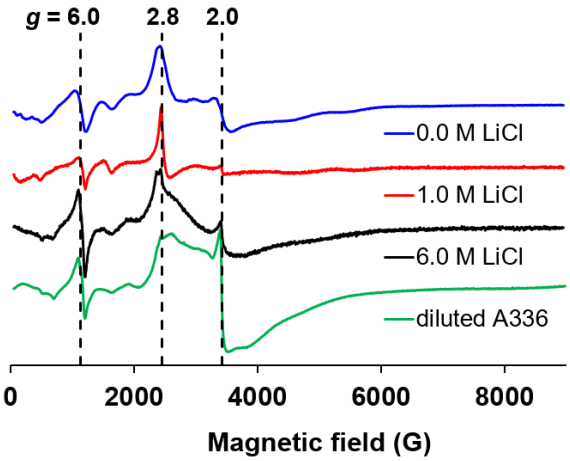

Figure S20. EPR spectra of Gd^{III} in methanolic solutions and in loaded LP phases recorded at 140 K.

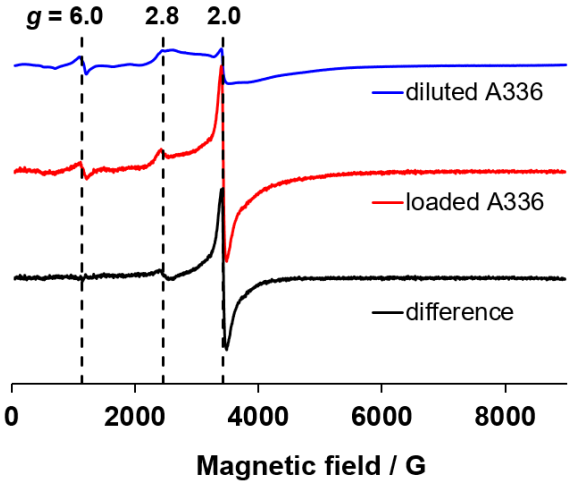

Figure S21. Comparison of Gd^{III} EPR spectra for undiluted and diluted A336 solutions

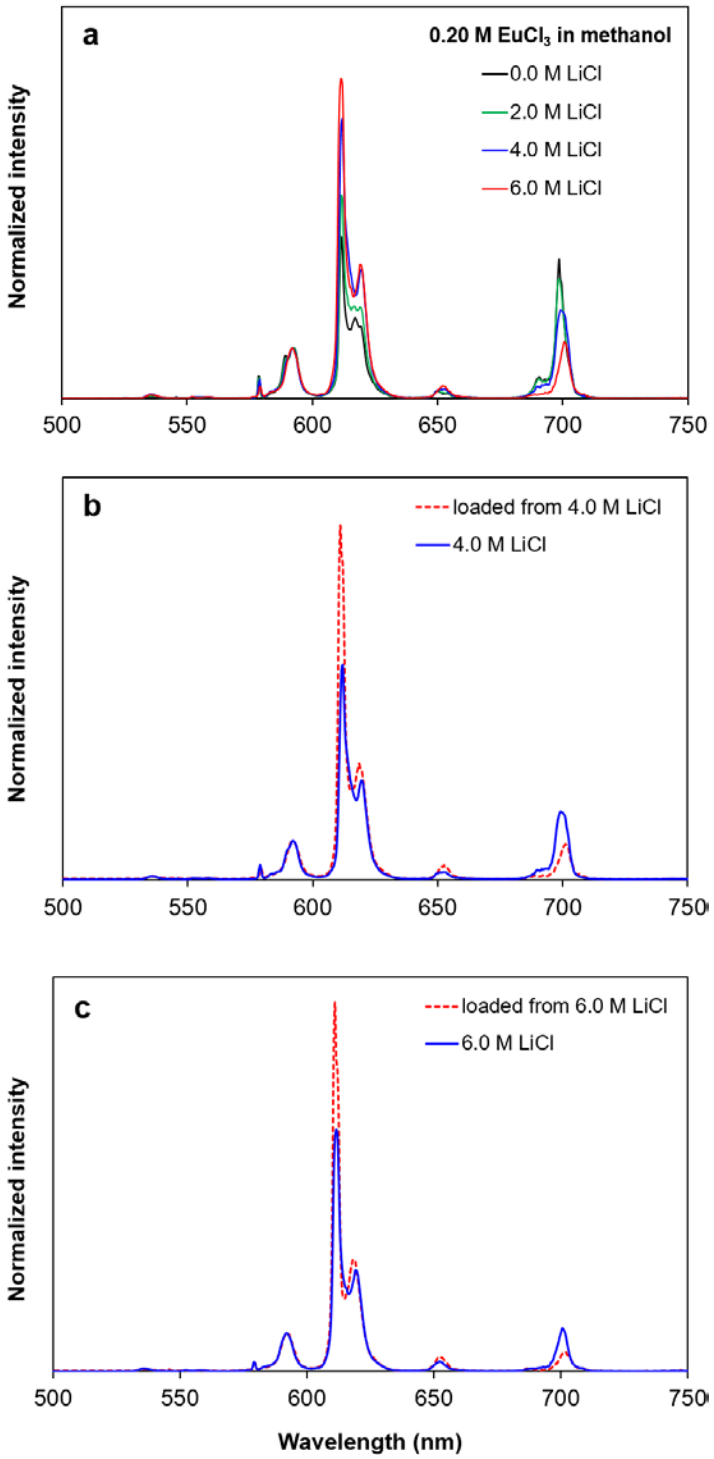

Figure S22. Emission spectra of Eu^{III} solutions: (a) 0.20 M $EuCl_3$ in methanol with various LiCl concentrations; (b) 0.20 M $EuCl_3$ and 4.0 M LiCl in methanol and the LP phase loaded from this methanolic solution; (c) 0.20 M $EuCl_3$ and 6.0 M LiCl in methanol and the LP phase loaded from this methanolic solution.

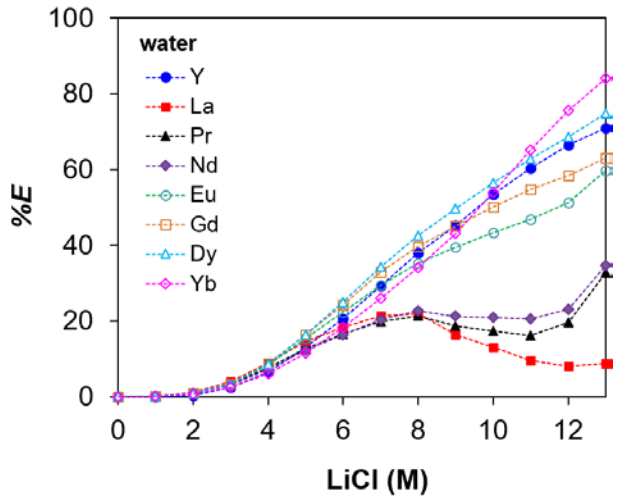

Figure S23. Extraction of rare-earth elements from aqueous solutions.

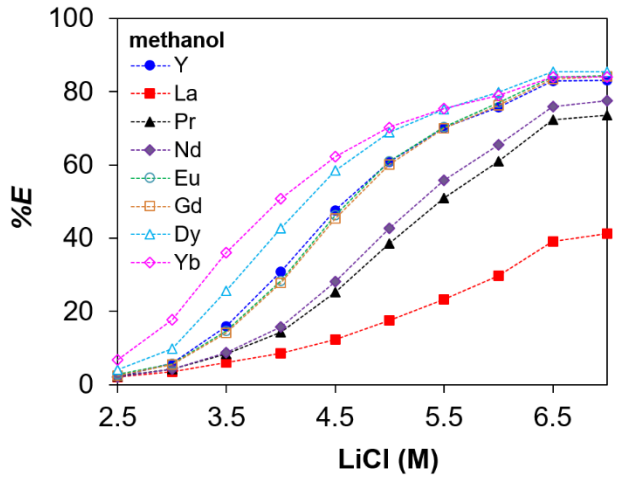

Figure S24. Extraction of rare-earth elements from methanolic solutions.

REFERENCES

[1] K. Larsson, C. Ekberg, A. Ødegaard-Jensen, *Hydrometallurgy.* **2012,** *129−130*, 35−42.

[2] T. Müller, B. Friedrich, *J. Power Sources* **2006**, *158*, 1498−1509.

[3] M. J. Frisch, G. W. Trucks, H. B. Schlegel, G. E. Scuseria, M. A. Robb, J. R. Cheeseman, G. Scalmani, V. Barone, B. Mennucci, G. A. Petersson, H. Nakatsuji, M. Caricato, X. Li, H. P. Hratchian, A. F. Izmaylov, J. Bloino, G. Zheng, J. L. Sonnenberg, M. Hada, M. Ehara, K. Toyota, R. Fukuda, J. Hasegawa, M. Ishida, T. Nakajima, Y. Honda, O. Kitao, H. Nakai, T. Vreven, J. A. Montgomery, Jr., J. E. Peralta, F. Ogliaro, M. Bearpark, J. J. Heyd, E. Brothers, K. N. Kudin, V. N. Staroverov, T. Keith, R. Kobayashi, J. Normand, K. Raghavachari, A. Rendell, J. C. Burant, S. S. Iyengar, J. Tomasi, M. Cossi, N. Rega, J. M. Millam, M. Klene, J. E. Knox, J. B. Cross, V. Bakken, C. Adamo, J. Jaramillo, R. Gomperts, R. E. Stratmann, O. Yazyev, A. J. Austin, R. Cammi, C. Pomelli, J. W. Ochterski, R. L. Martin, K. Morokuma, V. G. Zakrzewski, G. A. Voth, P. Salvador, J. J. Dannenberg, S. Dapprich, A. D. Daniels, O. Farkas, J. B. Foresman, J. V. Ortiz, J. Cioslowski, and D. J. Fox, Gaussian, *Gaussian 09, Revision E.01,* ; Gaussian, Inc., Wallingford CT, 2013.

[4] A. D. Becke, *J. Chem. Phys.* **1993**, *98*, 1372−1377.

[5] F. Weigend, R. Ahlrichs, *Phys. Chem. Chem. Phys.* **2005**, *7*, 3297−3305.

[6] E. A. Galván-García, E. Agacino-Valdés, M. Franco-Pérez, R. Gómez-Balderas, *Theor. Chem. Acc.* **2017**, *136*, 1−14.

[7] K. Fujii, Y. Umebayashi, R. Kanzaki, D. Kobayashi, R. Matsuura, S. Ishiguro, *J. Solution Chem.* **2005**, *34*, 739−753.

[8] M. Akihisa, *Bull. Chem. Soc. Jpn.* **1959**, *32*, 1381−1383.

[9] D. Knetsch, W. L. Groeneveld, *Inorg. Chim. Acta* **1973**, *7*, 81−87.

[10] D. Knetsch, W. L. Groeneveld, *Inorg.Nucl. Chem. Lett.* **1976**, *12*, 27−32.

[11] P. B. Lond, P. S. Salmon, D. C. Champeney, *J. Am. Chem. Soc.* **1991**, *113*, 6420−6425.

[12] C. M. Grgicak, R. G. Green, J. B. Giorgi, *J. Mater. Chem.* **2006**, *16*, 885−897.

[13] N. A. Matwiyoff, *Inorg. Chem.* **1966**, *5*, 788−795.

[14] J. F. Hinton, E. S. Amis, *Chem. Rev.* **1967**, *67*, 367−425.

[15] Y. Inada, H. Hayashi, K.-i. Sugimoto, S. Funahashi, *J. Phys. Chem. A* **1999**, *103*, 1401−1406.

[16] K. Fujii, Y. Matsumoto, Y. Kaieda, D. Kobayashi, Y. Umebayashi, S. Ishiguro, *J. Therm. Anal. Calorim.* **2006**, *85*, 567−573.

[17] H. Yokoyama, K. Nakajima, *J. Solution Chem.* **2004**, *33*, 607−629.

[18] BASF. *Aliquat 336*. 2013.

[19] A. Chiboub-Fellah, J. Meullemeestre, C. Spies, F. Vierling, M. A. Khan, *Transition Met. Chem. (London)* **1999**, *24*, 135−140.

[20] T. Vander Hoogerstraete, E. R. Souza, B. Onghena, D. Banerjee, K. Binnemans, *J. Solution Chem.* **2018**, *47*, 1351-1372.

[21] T. Yaita, H. Narita, S. Suzuki, S. Tachimori, H. Motohashi, H. J. Shiwaku, *Radioanal. Nucl. Chem.* 1999, 239, 371−375.

[22] A. A. Migdisov, A. E. Williams-Jones, C. Normand, S. A. Wood, *Geochim. Cosmochim. Acta*. 2008, 72, 1611−1625.

[23] J. R. Haas, E. L. Shock, D. C. Sassani, *Geochim. Cosmochim. Acta* 1995, 59, 4329−4350.

[24] S. A. Wood, *Chem. Geol.* **1990,** *82*, 159−186.

[25] K. S. Pitzer, *J. Phys. Chem.* **1973**, *77*, 268−277.

[26] K. S. Pitzer, *Activity coefficients in electrolyte solutions.* 2nd Edition, CRC Press, Inc., Boca Raton, Florida, **1991**.

[27] Y. Marcus, *Ions in Solution and their Solvation*, John Wiley & Sons, Inc., New Jersey, **2015**.

[28] C.-C. Chen, L. B. Evans, *AIChE J.* **1986**, *32*, 444−454.

[29] Y. Song, C.-C. Chen, *Ind. Eng. Chem. Res.* **2009**, *48*, 7788−7797.

[30] Y. Nagaosa, Y. Binghua, *Sep. Sci. Technol.* **1997**, *32*, 1053−1065.

[31] P. Zhang, T. Yokoyama, O. Itabashi, Y. Wakui, T. M. Suzuki, K. Inoue, *J. Power Sources* **1999**, *77*, 116−122.

[32] K. Larsson, C. Ekberg, A. Ødegaard-Jensen, *Hydrometallurgy* **2012,** *129−130*, 35−42.

[33] B. R. Reddy, D. N. Priya, *J. Power Sources* **2006**, *161*, 1428−1434.

[34] C. Tunsu, C. Ekberg, M. Foreman, T. Retegan, *Solvent Extr. Ion Exch.* **2014**, *32*, 650−668.

[35] T. Vander Hoogerstraete, S. Wellens, K. Verachtert, K. Binnemans, *Green Chem.* **2013**, *15*, 919−927.

[36] S. Raiguel, D. Depuydt, T. Vander Hoogerstraete, J. Thomas, W. Dehaen, K. Binnemans, *Dalton Trans.* **2017**, *46*, 5269−5278.

[37] L. S. Smith, D. C. McCain, D. L. Wertz, *J. Am. Chem. Soc.* **1976**, *98*, 5125−5128.

[38] A. Burakowski, J. Gliński, J. Wachał, M. Guzik, *Chem. Phys*. **2015**, *463*, 5−9.

[39] H. B. Silber, D. Bouler, T. White, *J. Phys. Chem*. **1978**, *82*, 775−779.

[40] H. B. Silber, T. Mioduski, *Inorg. Chem*. **1984**, *23*, 1577−1583.

[41] M. L. Steele, D. L. Wertz, *Inorg. Chem*. **1977**, *16*, 1225−1228.

[42] M. Hamze, J. Meullemeestre, M. J. Schwing, F. Vierling, *J. Less Common Met.* **1986,** *118*, 153−166.

[43] S. Stoll, A. Schweiger, *J. Magn. Reson.* **2006**, *178*, 42−55.

[44] M. Mazur, P. Poprac, M. Valko, C. J. Rhodes, *J. Sol-Gel Sci. Technol*. **2016**, *79*, 220−227.

[45] C. M. Brodbeck, L. E. Iton, *J. Chem. Phys*. **1985**, *83*, 4285−4299.

[46] C. Platas-Iglesias, L. Vander Elst, W. Zhou, R. N. Muller, C. F. G. C. Geraldes, T. Maschmeyer, J. A. Peters, *Chem. Eur. J.* **2002**, *8*, 5121−5131.

[47] K. Binnemans, *Coord. Chem. Rev*. **2015**, *295*, 1−45.

[48] C. Görller-Walrand, N. D. Moitié-Neyt, Y. Beyens, J. C. Bünzli, *J. Chem. Phys.* **1982**, *77*, 2261−2265.

[49] Solvents. http://gaussian.com/scrf/. Accessed on 5 April 2019.